



Performance Enhancement of a Ventilated Grass Tray for Rooftop Thermal Reduction

Thana Ananacha ^{*}, Anon Anan-archa 

Faculty of Architecture and Design, King Mongkut's University of Technology North Bangkok, Bangkok 10800, Thailand

Corresponding Author Email: thana.a@archd.kmutnb.ac.th

Copyright: ©2026 The authors. This article is published by IETA and is licensed under the CC BY 4.0 license (<http://creativecommons.org/licenses/by/4.0/>).

<https://doi.org/10.18280/ijht.440112>

ABSTRACT

Received: 1 October 2025

Revised: 29 December 2025

Accepted: 9 January 2026

Available online: 28 February 2026

Keywords:

grass tray system, ventilated roofing, passive cooling, heat gain reduction, air change rate, rooftop thermal performance, natural ventilation, experimental field testing

This study evaluates the thermal performance of two modular rooftop grass tray systems for passive cooling in tropical climates. A baseline Ventilated Grass Tray (VGT) and an enhanced Multi-Tube Connected Ventilated Grass Tray (MCVGT) were developed to examine how integrated passive ventilation influences sub tray airflow and heat dissipation. Three test chambers, including a bare roof reference VGT and MCVGT, were installed on an exposed rooftop in Bangkok, Thailand, and monitored under real tropical outdoor conditions during a continuous 10 hour daytime period from 08:00 to 18:00. Key parameters included sub tray temperature rooftop surface temperature, ceiling heat flux, indoor air temperature airflow rate, and air change characteristics. The MCVGT system demonstrated consistently lower sub tray and rooftop surface temperatures due to strengthened buoyancy driven convection enabled by multiple vertical tubes and interconnected perimeter openings. Ceiling and indoor air temperatures were also reduced with the MCVGT room maintaining conditions close to ambient levels. Airflow measurements showed that the MCVGT achieved higher airflow rates and air change values reaching approximately 7 h^{-1} during peak solar periods, while the VGT reached approximately 2 h^{-1} . Heat flux analysis indicated substantial reductions in conductive heat gain compared with both the VGT and bare roof conditions. These findings confirm that incorporating enhanced ventilation pathways into lightweight rooftop greenery systems can improve passive cooling performance and provide a practical energy efficient solution for tropical urban buildings.

1. INTRODUCTION

Urban areas in tropical regions experience severe rooftop heat accumulation due to high solar exposure, elevated humidity, and persistent outdoor temperatures that often exceed 32 to 35 °C. This excess rooftop heating intensifies conductive heat transfer into buildings and leads to elevated indoor temperatures. As a consequence, reliance on mechanical cooling systems increases significantly [1]. Such dependence on air conditioning results in higher energy consumption and greater environmental burdens [2]. For this reason, passive and nature based rooftop cooling strategies have become increasingly important for sustainable urban development.

Green roofs have been widely recognized for their ability to enhance urban sustainability [3, 4]. Their cooling performance is primarily associated with shading evapotranspiration and thermal buffering provided by vegetation and substrate layers [5, 6]. Extensive research indicates that green roofs can effectively reduce rooftop heat gain, improve local microclimatic conditions, and contribute to long term environmental benefits [7, 8]. Beyond thermal performance, rooftop greenery also supports food production, ecological diversity, and social well being. These additional benefits further strengthen the role of green roofs as a central nature based strategy for climate responsive urban design [9, 10].

However, the cooling effectiveness of green roofs in hot and humid tropical climates remains limited. High substrate moisture content, combined with restricted evapotranspiration efficiency, reduces the ability of vegetation layers to dissipate heat under humid atmospheric conditions. As a result, rooftop temperatures may remain elevated during peak solar hours [11-13]. In addition, many buildings in Southeast Asia rely on lightweight structural systems. These buildings often require modular or low load rooftop solutions, which limit the applicability of conventional green roof assemblies [14]. These combined constraints indicate a clear need for improved green roof configurations that are better suited to tropical climatic characteristics and structural limitations.

Parallel research on passive ventilation systems provides valuable insights for enhancing rooftop thermal performance. Studies on façade ventilation, balcony airflow, ventilated walls, tile ventilators, solar chimneys, and light vent pipe systems consistently demonstrate that engineered airflow pathways can promote buoyancy driven ventilation [15-17]. This mechanism enables effective removal of accumulated heat from building envelopes [18-20]. Although these studies confirm the effectiveness of ventilation driven heat removal, they are primarily focused on roof or façade ventilation devices rather than vegetation based rooftop systems [21-25]. Similarly, most green roof studies emphasize shading effects, substrate thermal mass, and evapotranspiration performance

while giving limited attention to the role of engineered airflow beneath planting layers. As a result, the integration of passive ventilation mechanisms into modular grass tray systems has not been systematically investigated.

Despite this potential, most modular green roof trays lack designed ventilation pathways. Their sub tray air spaces often remain stagnant, which limits natural convection and prevents effective heat removal, particularly under intense tropical solar radiation. To date, experimental studies that specifically evaluate the thermal and airflow performance of modular Ventilated Grass Tray (VGT) systems under real tropical rooftop conditions remain scarce. This limitation represents a clear research gap.

To address this gap, the present study introduces an enhanced modular grass tray system with integrated passive ventilation mechanisms. The first configuration represents the baseline VGT. This system incorporates a sloped undertray cavity and a limited number of vertical ducts, which allow only modest upward airflow. The second configuration, referred to as the Multi-Tube Connected Ventilated Grass Tray (MCVGT), includes a greater number of ventilation tubes together with interconnected perimeter openings. These features promote continuous lateral and vertical airflow beneath the tray system. The proposed design improvements are intended to intensify buoyancy driven convection, reduce heat accumulation within the sub tray cavity, and enhance both rooftop and indoor thermal performance.

The objective of this research is to evaluate and compare the thermal performance and ventilation behavior of the VGT and MCVGT systems under real tropical rooftop conditions. Field measurements were conducted to assess sub tray temperature, rooftop surface temperature, ceiling heat flux, indoor air temperature, airflow rate, and air change characteristics. The findings contribute to the advancement of lightweight energy efficient and climate responsive rooftop cooling systems suitable for densely built tropical cities.

To clarify the scientific scope of the study, the investigation focuses on two main aspects. First, the study examines whether the integration of additional ventilation pathways in the MCVGT leads to higher sub tray airflow rates and air change characteristics when compared with the VGT under identical rooftop exposure conditions. Second, the study evaluates whether the enhanced ventilation performance of the MCVGT results in measurable reductions in rooftop surface temperature, ceiling heat flux, and indoor air temperature relative to the VGT and bare roof configurations. Based on buoyancy driven ventilation principles, the working hypothesis of this study is that increasing both the number of vertical ventilation tubes and the continuity of lateral airflow pathways beneath the grass trays intensifies natural convection. This enhanced convective airflow is expected to generate higher air change rates and improved rooftop thermal reduction performance.

2. DESIGN CONFIGURATION AND VENTILATION MECHANISM OF THE GRASS TRAYS

Two modular rooftop grass tray configurations were developed to investigate how passive ventilation design influences thermal and airflow performance. Both tray types share the same external dimensions of 0.30×0.30 m with a height of 0.04 m and are fabricated from 3 mm PVC foam board (Plastwood), selected for its durability, low weight, and

structural rigidity suitable for rooftop installation. Each tray contains a 20 mm planting layer filled with dwarf Malaysian grass (*Axonopus compressus*), a species chosen for its heat tolerance and shallow root system that aligns well with lightweight rooftop applications. The overall configurations and structural characteristics of the two grass tray systems are illustrated in Figure 1.

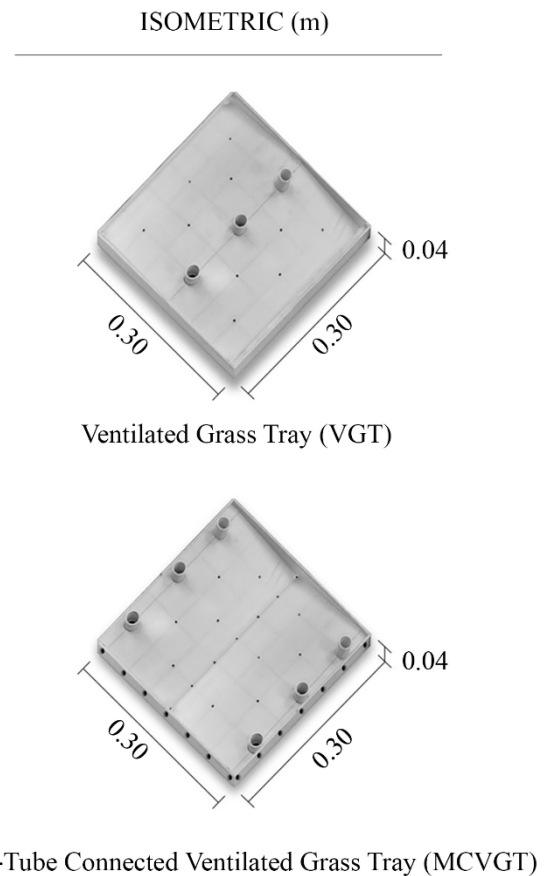


Figure 1. The two types of grass trays used in the experiment

2.1 Baseline Ventilated Grass Tray (VGT)

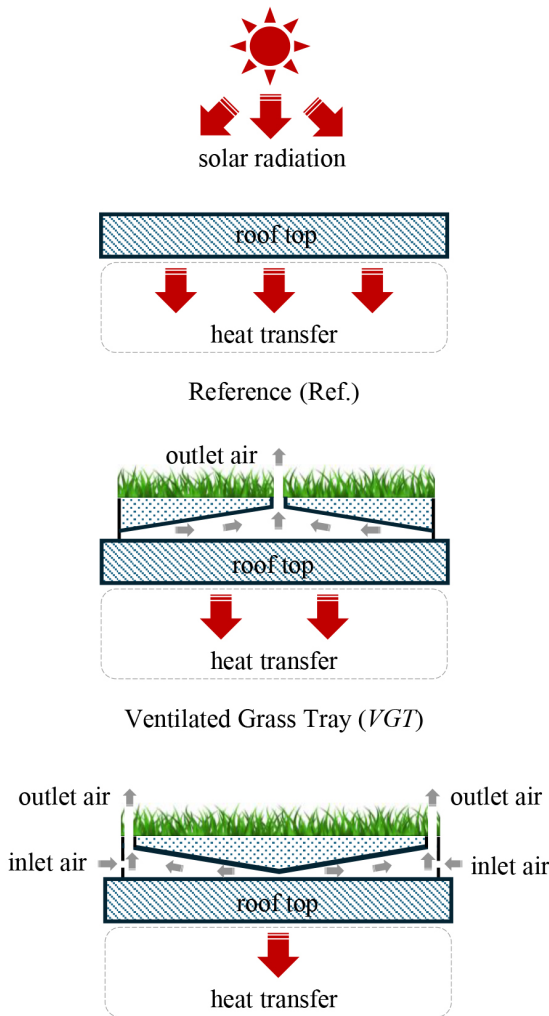
The first configuration represents the baseline VGT. Its design incorporates a 12° gable-shaped base that promotes water runoff while creating a stable air cavity beneath the tray. This cavity functions as a passive insulation layer by reducing direct conductive heat transfer from the heated roof surface to the planting substrate. Vertically oriented cylindrical ventilation tubes extend through the tray body, linking the air cavity to the outdoor environment. When heated air in the cavity rises due to solar radiation, these ducts provide pathways for upward exhaust, inducing the inflow of cooler ambient air from the tray edges. The resulting buoyancy-driven movement supports convective heat dissipation. Raised tray edges contain the soil and maintain structural stability without obstructing vertical airflow.

2.2 Multi-Tube Connected Ventilated Grass Tray (MCVGT)

The second configuration, known as the MCVGT, incorporates several enhancements intended to strengthen natural convection beneath the tray. Although its overall dimensions and material properties remain identical to the

VGT, the MCVGT features a 12° butterfly-shaped base that increases the cross-sectional space available for air movement. The number of vertical ventilation tubes is increased, and their distribution is optimized on both sides of the tray to support greater upward airflow. In addition to these vertical ducts, perforated openings are positioned along all four tray edges. These perimeter openings interconnect the sub-tray air spaces of adjacent trays, enabling continuous lateral airflow across the rooftop assembly. The resulting network of vertical and horizontal pathways substantially improves ventilation continuity and enhances the overall effectiveness of convective cooling beneath the vegetation layer.

GRASS TRAYS SECTION



Multi-Tube Connected Ventilated Grass Tray (MCVGT)

Figure 2. Schematic diagram of airflow and thermal dissipation in Ventilated Grass Tray (VGT) and Multi-Tube Connected Ventilated Grass Trays (MCVGT)

2.3 Ventilation mechanism of both systems

Both tray configurations rely on buoyancy-driven natural convection as the primary mechanism governing airflow beneath the planting substrate. Solar heating elevates the temperature of the rooftop surface and the sub-tray cavity, reducing the density of trapped air and initiating upward movement. In the VGT, the sloped cavity and limited vertical tubes provide a moderate outlet for rising warm air, resulting in modest convective flow. In contrast, the MCVGT's

expanded set of ventilation tubes and perimeter openings establishes multiple inlet and outlet pathways that support continuous and multidirectional air circulation. This improved ventilation mechanism enhances convective heat removal, lowers temperature buildup within the planting layer, and reduces the overall rooftop heat load. A conceptual representation of airflow patterns for both systems is illustrated in Figure 2.

3. EXPERIMENTAL SETUP

3.1 Test chambers and rooftop installation

Field experiments were conducted using three insulated test chambers installed on an exposed flat rooftop to ensure uniform environmental conditions. Each chamber had an internal volume of 1.215 m³ and was constructed with lightweight insulated wall panels to minimize lateral heat exchange. The rooftop of each chamber was designed as a reinforced flat assembly capable of supporting the weight of nine modular grass trays while maintaining consistent thermal characteristics across all test units.

Three rooftop configurations were examined: a bare-roof reference chamber with no vegetation, a chamber fitted with nine baseline VGTs, and a chamber equipped with nine MCVGTs. The chambers were positioned adjacent to each other to guarantee identical exposure to solar radiation, wind, and outdoor climatic variations throughout the experimental period. The rooftop installation layout and field exposure conditions of the three test chambers are shown in Figure 3.



Figure 3. Rooftop exposure of reference, Ventilated Grass Tray (VGT), and Multi-Tube Connected Ventilated Grass Trays (MCVGT) test rooms under field conditions

3.2 Instrumentation

A comprehensive sensor system was deployed to monitor thermal, radiative, and ventilation parameters. K-type thermocouples (temperature range 0–1250 °C, accuracy ±0.5 °C) were installed at the geometric center of the indoor air volume of each chamber and within the sub-tray cavities to continuously record indoor and cavity temperatures. A heat flux sensor (Omega HFS-3; measurement range 1–1400 W/m², accuracy ±0.5%) was embedded beneath the interior ceiling surface to quantify downward conductive heat transfer into the room. Solar radiation was measured using an EKO ML-01

silicon pyranometer (sensitivity $15 \mu\text{V}/\text{W}\cdot\text{m}^2$, accuracy $\pm 5\%$), mounted on top of the reference chamber's roof. Airflow velocities in both the VGT and MCVGT systems were recorded using a hot-wire anemometer (TSI Model 8380; range 0–50 m/s, accuracy $\pm 0.5\%$). Measurements were obtained at inlet openings, interconnecting perimeter openings (MCVGT only), and the vertical exhaust tubes to capture buoyancy-driven airflow patterns. The detailed sensor locations and measurement positions for all monitored parameters in the Ref., VGT, and MCVGT test chambers are illustrated in Figure 4.

All instruments were connected to a Hioki 8422-52 data logger (accuracy $\pm 0.8\%$), enabling synchronized, multi-channel data acquisition for the entire experiment.

3.3 Measurement period and operating conditions

Measurements were recorded simultaneously for all three chambers over a continuous 10-hour daytime period from 08:00 to 18:00. Data were logged every 30 minutes to capture diurnal variations under changing solar intensities.

To ensure consistent vegetation and moisture conditions, the grass trays in both VGT and MCVGT systems were watered daily at 07:00. The monitored variables included sub-tray air temperature, rooftop surface temperature, indoor air temperature, ceiling surface temperature, outdoor ambient temperature, ceiling heat flux, airflow velocity at all

ventilation openings, and solar radiation intensity. These parameters formed the basis for comparing thermal and ventilation performance between the two tray configurations.

3.4 Calculation of airflow and air exchange rate

The volumetric airflow rate generated by buoyancy-driven convection in the grass tray ventilation ducts was determined based on Eq. (1):

$$Q = A \cdot v \quad (1)$$

where, Q is the airflow rate, m^3/s , A is the cross-sectional area of the ventilation opening, m^2 , and v is the measured air velocity, m/s , at the outlet of the vertical tubes.

The corresponding air change per hour (ACH) within the sub-tray air cavity was calculated using the following Eq. (2):

$$ACH = \frac{3600Q}{V} \quad (2)$$

where, V represents the volume of the air cavity, m^3 , and 3600 is the number of seconds in one hour. These calculations were applied to both the VGT and MCVGT systems to quantify their passive ventilation effectiveness and to assess differences in buoyancy-driven airflow behavior resulting from their respective design configurations.

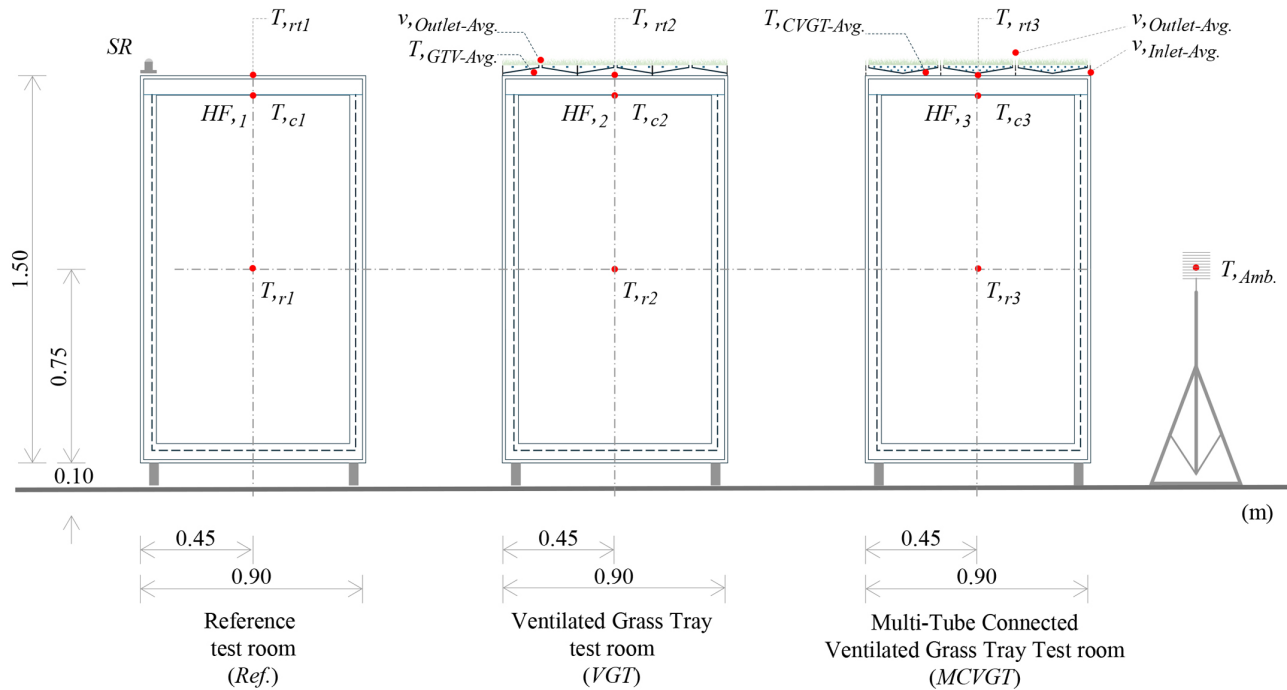


Figure 4. Measured positions of Reference, Ventilated Grass Tray (VGT), and Multi-Tube Connected Ventilated Grass Trays (MCVGT) test room

4. RESULTS AND DISCUSSION

The thermal and ventilation performance of the grass tray systems was evaluated under real outdoor conditions over a continuous 10-hour daytime period. Results from the three test chambers, the bare roof (reference), VGT, and MCVGT, are presented in relation to temperature profiles, airflow characteristics, and heat gain behavior. The analyses emphasize both instantaneous diurnal responses and averaged

thermal trends to clarify the mechanisms by which the MCVGT system improves rooftop thermal performance.

4.1 Temperature profiles

4.1.1 Air gap temperature in grass trays

Figure 5 presents the hourly variations of air temperature within the sub-tray cavities of the VGT and MCVGT systems compared with the outdoor ambient temperature. Both tray

configurations exhibited a steady temperature rise shortly after sunrise, driven primarily by increasing solar irradiance. The cavity temperature in the VGT system reached a peak of approximately 41 °C between 13:00 and 14:00, whereas the MCVGT system maintained slightly lower peak values throughout the same period.

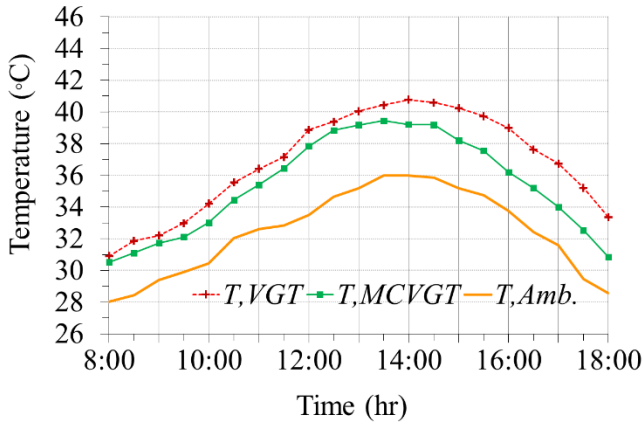


Figure 5. Hourly variations in air gap temperatures of the Ventilated Grass Tray (VGT) and Multi-Tube Connected Ventilated Grass Trays (MCVGT) systems compared to ambient temperature

As summarized in Table 1, the average cavity temperature of the VGT system was 36.82 °C, while the MCVGT system recorded a lower average of 35.38 °C. This represents a reduction of 1.44 °C attributable to the enhanced ventilation pathways incorporated in the MCVGT design. When compared against the ambient average temperature of 32.41 °C, the excess temperature above ambient was 4.42 °C for the VGT and 2.98 °C for the MCVGT.

These results indicate that the additional vertical ventilation tubes and interconnected perimeter openings in the MCVGT system effectively promote heat removal from the sub-tray cavity. The strengthened buoyancy-driven airflow reduces thermal accumulation and contributes to more stable sub-tray thermal conditions under tropical rooftop exposure.

Table 1. Comparison of average air gap temperatures and temperature differences relative to ambient air in Ventilated Grass Tray (VGT) and Multi-Tube Connected Ventilated Grass Tray (MCVGT) systems

Air gab/ Ambient Temp.	Average Temp. (°C)	Comparison Temp.	Difference Temp. (°C)
T, VGT	36.82	T, VGT - T, MCVGT	1.44
T, MCVGT	35.38	T, MCVGT - T, amb.	2.98
T, Amb.	32.41	T, VGT - T, amb.	4.42

4.1.2 Rooftop surface temperatures

Figure 6 illustrates the hourly rooftop surface temperatures measured for the three test configurations: the bare-roof reference, the VGT system, and the MCVGT system, together with the ambient air temperature. All configurations exhibited a similar diurnal heating trend, with surface temperatures increasing from 08:00 onwards and reaching maximum values in the early afternoon, between 13:00 and 14:00. During the morning period (08:00–11:00), the differences among the three roofs were still moderate, reflecting the combined effects of gradually rising solar radiation and relatively low

accumulated heat within the roof assemblies.

As solar irradiance intensified toward midday, the thermal behavior of each configuration became more distinct. The reference bare roof, which was directly exposed to solar radiation without any shading or additional insulation, recorded the highest peak rooftop temperature of 44.45 °C. This elevated temperature clearly indicates strong heat absorption at the outer surface, which is subsequently conducted into the interior space. In contrast, both grass tray systems substantially reduced rooftop surface temperatures due to the combined effects of shading by vegetation, thermal buffering in the planting medium, and, in the case of ventilated systems, convective heat removal from the sub-tray cavity.

The VGT system reduced the peak rooftop temperature to 41.77 °C, demonstrating the benefit of adding a grass tray with an air gap beneath the planting layer. The MCVGT system performed even better, achieving the lowest peak rooftop temperature of 40.37 °C. This additional reduction can be attributed to the enhanced ventilation pathways in the MCVGT, which promote buoyancy-driven airflow and facilitate the removal of accumulated heat beneath the tray.

Daily average temperatures further emphasize these differences. As summarized in Table 2, the average rooftop temperatures were 39.10 °C for the reference roof, 37.50 °C for the VGT, and 36.10 °C for the MCVGT. Thus, the MCVGT roof was 1.40 °C cooler than the VGT and 3.00 °C cooler than the bare roof over the 10-hour monitoring period. When compared to the ambient average temperature of 32.41 °C, the MCVGT rooftop surface was only 3.70 °C higher, indicating that the combined effects of shading and enhanced sub-tray ventilation significantly limit net heat absorption at the roof surface.

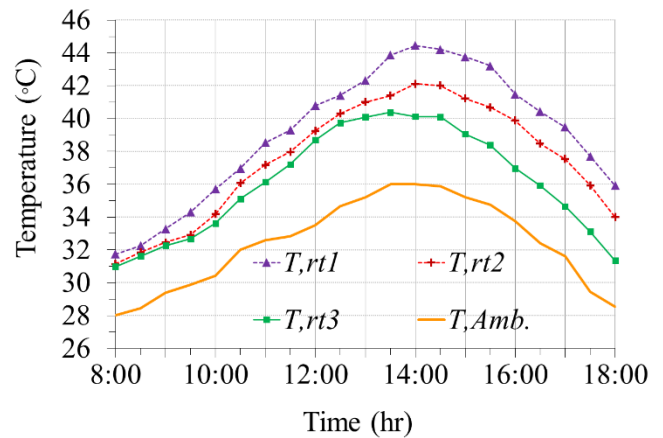


Figure 6. Hourly variation of rooftop surface temperatures ($T_{,rt1}$, $T_{,rt2}$, $T_{,rt3}$) and ambient temperature ($T_{,Amb.}$)

Table 2. Comparison of average rooftop temperatures and comparative differences among Ventilated Grass Tray (VGT), Multi-Tube Connected Ventilated Grass Tray (MCVGT), and reference configurations

Rooftop/ Ambient Temp.	Average Temp. (°C)	Comparison Temp.	Difference Temp. (°C)
$T_{,rt1}$	39.10	$T_{,rt1} - T_{,rt2}$	1.60
$T_{,rt2}$	37.50	$T_{,rt2} - T_{,rt3}$	1.40
$T_{,rt3}$	36.10	$T_{,rt1} - T_{,rt3}$	3.00
$T_{,Amb.}$	32.41	$T_{,rt3} - T_{,Amb.}$	3.70

Overall, these results confirm that the integration of multi-tube connected ventilation within the grass tray system provides an incremental improvement over the conventional ventilated tray. By lowering rooftop surface temperatures throughout the day, particularly during peak solar hours, the MCVGT configuration effectively reduces the driving temperature gradient for conductive heat transfer into the building, thereby supporting subsequent reductions in ceiling surface temperature and indoor air temperature discussed in the following sections.

4.1.3 Ceiling surface temperatures

Figure 7 presents the hourly ceiling surface temperatures measured inside the three test rooms: the bare-roof reference chamber, the chamber equipped with VGT trays, and the chamber fitted with MCVGT trays. The ceiling temperature is a key indicator of conductive heat transfer through the roof structure and directly influences indoor thermal conditions. Across all configurations, ceiling temperatures increased gradually from the morning period and reached their highest values between 13:00 and 14:00, corresponding to the period of maximum rooftop heat loading. The reference room, which had no shading or sub-tray ventilation system, recorded the highest ceiling temperatures throughout the day. Its peak ceiling temperature approached 41 °C, reflecting strong conductive heat transfer from the highly heated roof surface. This behavior aligns with the rooftop surface temperature profile, where the bare roof exhibited the highest solar heat absorption. The VGT-equipped room showed a noticeable improvement, with ceiling temperatures consistently lower than the reference room during both morning and afternoon periods. This reduction can be attributed to the shading effect provided by vegetation and the thermal buffering capacity of the substrate and air gap beneath the trays. These features help to delay and diminish the amount of heat conducted to the ceiling.

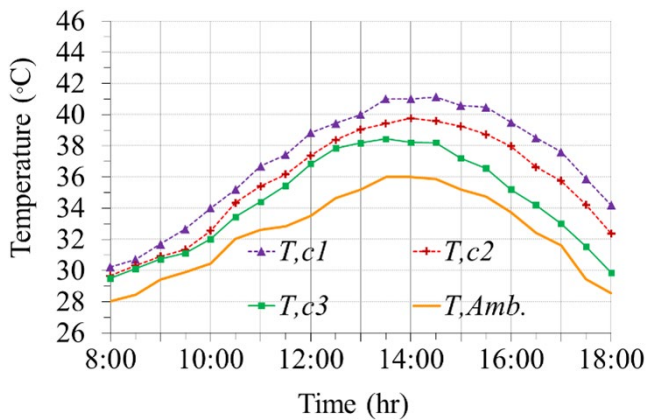


Figure 7. Hourly variations in ceiling temperatures under different rooftop configurations: T_{c1} (reference), T_{c2} (Ventilated Grass Tray (VGT)), and T_{c3} (Multi-Tube Connected Ventilated Grass Trays (MCVGT))

The MCVGT system delivered the greatest reduction in ceiling surface temperature. Throughout the monitoring period, the MCVGT ceiling remained the coolest among the three configurations. This enhanced performance stems from the system’s improved ventilation design, which promotes continuous buoyancy-driven airflow beneath the trays. By actively transporting warm air out of the sub-tray cavity, the MCVGT minimizes heat accumulation at the rooftop interface,

resulting in less conductive heat transmitted downward.

As summarized in Table 3, the average ceiling temperature of the reference room was 36.99 °C, compared with 35.68 °C for the VGT room and 34.38 °C for the MCVGT room. This represents a 1.31 °C reduction between the reference and VGT rooms, and a further 1.30 °C reduction between the VGT and MCVGT rooms. The total decrease of 2.61 °C between the reference and MCVGT configurations highlights the effectiveness of integrating enhanced ventilation into the grass tray design.

In addition, when the MCVGT ceiling temperature is compared with the ambient average temperature of 32.41 °C, the difference is only 1.98 °C, suggesting that the system significantly limits heat transfer into the indoor space even during periods of intense solar radiation. These findings demonstrate that improvements in sub-tray ventilation not only reduce rooftop surface temperatures but also provide important downstream benefits for indoor thermal comfort and energy efficiency.

Table 3. Average ceiling temperatures and temperature differences for Ventilated Grass Tray (VGT), Multi-Tube Connected Ventilated Grass Trays (MCVGT), and reference rooms compared to ambient air

Ceiling/ Ambient Temp.	Average Temp. (°C)	Comparison Temp.	Difference Temp. (°C)
T_{c1}	36.99	$T_{c1} - T_{c2}$	1.31
T_{c2}	35.68	$T_{c2} - T_{c3}$	1.30
T_{c3}	34.38	$T_{c1} - T_{c3}$	2.61
T_{Amb}	32.41	$T_{r3} - T_{Amb}$	1.98

4.1.4 Indoor air temperatures

Figure 8 illustrates the hourly indoor air temperatures recorded in the three test chambers: the bare-roof reference room, the VGT-equipped room, and the MCVGT-equipped room. Indoor air temperature reflects the cumulative effect of rooftop surface heating, ceiling heat transfer, and the moderating influence of vegetation and ventilation systems. Consistent with the patterns observed in rooftop and ceiling surface temperatures, the reference room recorded the highest indoor temperatures throughout the monitoring period, with a peak value of 38.54 °C during early afternoon. This elevated temperature highlights the strong downward heat flow from the unshaded roof and its direct impact on indoor thermal conditions.

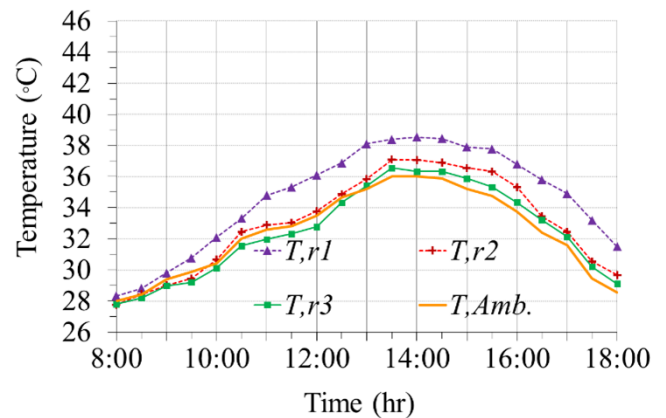


Figure 8. Hourly variations in indoor air temperatures of test rooms with different rooftop configurations: T_{r1} (reference), T_{r2} (Ventilated Grass Tray (VGT)), and T_{r3} (Multi-Tube Connected Ventilated Grass Trays (MCVGT))

The VGT system provided a clear improvement, lowering indoor air temperatures relative to the reference room during both morning and afternoon hours. Shading from the grass layer, coupled with the insulating air gap beneath the tray, helped reduce conductive heat transfer into the room. Peak indoor temperature in the VGT room reached 37.08 °C, noticeably lower than that of the reference room. The MCVGT system delivered the most pronounced cooling effect. Indoor temperatures in the MCVGT room remained consistently lower than in both the VGT and reference rooms throughout the day. This improvement reflects the combined influence of rooftop shading, substrate buffering, and enhanced convective heat removal through multi-directional airflow pathways in the MCVGT configuration. The stronger buoyancy-driven ventilation under higher solar radiation helped limit thermal buildup at the rooftop interface, leading to reduced heat transmission into the interior space.

As shown in Table 4, the afternoon average indoor temperature of the MCVGT room was 34.07 °C–0.59 °C lower than the VGT room and 2.42 °C lower than the reference room. During the morning period, the MCVGT room maintained an even narrower temperature range, with a maximum indoor temperature of 36.55 °C compared to 38.54 °C in the reference room. Table 5 further highlights that the MCVGT room achieved the lowest overall average indoor temperature (32.48 °C) over the full 10-hour monitoring period, which is only 0.07 °C above the ambient average temperature (32.41 °C). These findings demonstrate that the enhanced passive ventilation design of the MCVGT system plays a crucial role in stabilizing indoor thermal conditions. By reducing both rooftop surface temperatures and ceiling heat flux, the MCVGT minimizes indoor heat gain even under strong solar loading. This capability is particularly beneficial for buildings in tropical climates, where maintaining indoor temperatures closer to ambient levels can meaningfully reduce cooling energy demand.

Table 4. Average and maximum indoor temperatures of test rooms and ambient air during morning and afternoon periods

Room/ Ambient Temp.	Time	Average Temp. (°C)	Maximum Temp. (°C)
T_{r1}	08.00-13.00	33.12	38.54
	13.00-18.00	36.49	
T_{r2}	08.00-13.00	31.65	37.08
	13.00-18.00	34.66	
T_{r3}	08.00-13.00	31.15	36.55
	13.00-18.00	34.07	
$T_{Amb.}$	08.00-13.00	31.54	36.00
	13.00-18.00	33.52	

Table 5. Average indoor temperatures and differences among test rooms and ambient conditions

Room/ Ambient Temp.	Average Temp. (°C)	Comparison Temp.	Difference Temp. (°C)
T_{r1}	34.65	$T_{r1} - T_{r2}$	1.62
T_{r2}	33.03	$T_{r2} - T_{r3}$	0.55
T_{r3}	32.48	$T_{r1} - T_{r3}$	2.17
$T_{Amb.}$	32.41	$T_{r3} - T_{Amb.}$	0.07

4.2 Airflow and air change rate

Figure 9 presents the diurnal variation of airflow rates

generated by buoyancy driven ventilation in the VGT and MCVGT systems in relation to solar radiation intensity. In both configurations, airflow was initiated shortly after sunrise as solar heating increased the temperature difference between the sub tray air cavity and the ambient environment. During the early morning period, airflow rates remained relatively low due to limited thermal driving forces.

As solar radiation intensified toward midday, the airflow performance of the two systems became increasingly distinct. The VGT system exhibited a gradual increase in airflow corresponding to rising cavity temperatures. However, the magnitude of airflow remained limited throughout the day. This behavior is attributed to the restricted number of vertical ventilation tubes and the absence of continuous lateral airflow pathways beneath the trays. The limited outlet area and higher flow resistance constrained the development of strong buoyancy driven convection within the sub tray cavity.

In contrast, the MCVGT system demonstrated a more pronounced increase in airflow as solar radiation increased. The combined presence of multiple vertical ventilation tubes and interconnected perimeter openings substantially increased the effective ventilation area and reduced airflow resistance within the sub tray cavity. These design features promoted continuous lateral air movement between adjacent trays and facilitated more efficient upward exhaust through the vertical tubes. As a result, the buoyancy driven pressure difference generated under high solar loading produced higher volumetric airflow rates in the MCVGT system.

The calculated air change per hour values further illustrate this difference in ventilation effectiveness. The VGT system achieved air change rates of approximately 2 h⁻¹ during peak solar periods. In comparison, the MCVGT system reached air change values exceeding 7 h⁻¹ under similar environmental conditions. This increase in air change rate can be explained by the greater continuity of airflow pathways in the MCVGT, which enables rapid replacement of warm air within the sub tray cavity with cooler ambient air. The enhanced ventilation effectively limits thermal accumulation beneath the grass trays and supports sustained convective heat removal.

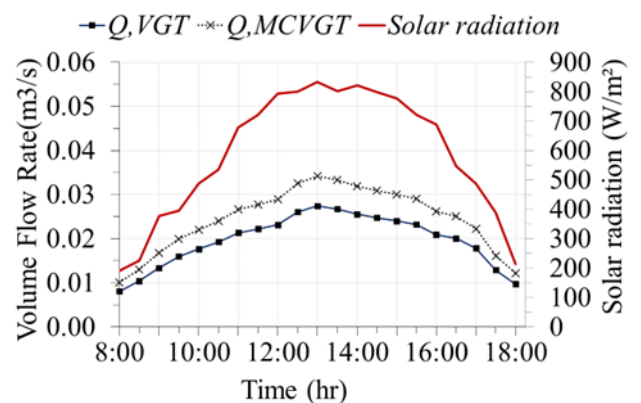


Figure 9. Hourly airflow performance of Ventilated Grass Tray (VGT) and Multi-Tube Connected Ventilated Grass Trays (MCVGT) systems in relation to solar irradiance

These results confirm that the higher air change performance of the MCVGT is not solely a consequence of increased solar heating but is directly linked to the engineered ventilation configuration. The synergistic interaction between vertical exhaust tubes and perimeter interconnected openings plays a critical role in intensifying buoyancy driven airflow.

This mechanism explains the substantial difference in air change characteristics observed between the MCVGT and VGT systems under identical rooftop exposure conditions.

4.3 Heat gain reduction

Figure 10 illustrates the hourly ceiling heat flux measured in the three test rooms, reference (bare roof), VGT, and MCVGT, together with the corresponding solar radiation intensity. The reference room consistently exhibited the highest heat flux throughout the day, peaking at approximately 148 W/m² during the early afternoon when solar radiation was at its maximum. This behavior reflects the strong conductive heat transfer through the unshaded roof structure, which experienced the highest rooftop temperatures among the three configurations. Both the VGT and MCVGT systems demonstrated significant reductions in ceiling heat flux compared with the bare roof. The reduction observed in the VGT room can be attributed to a combination of shading from vegetation, moderated roof surface temperatures, and partial thermal buffering provided by the sub-tray air gap. However, the MCVGT system achieved the most substantial reductions, reflecting its ability to limit heat accumulation more effectively through enhanced buoyancy-driven ventilation.

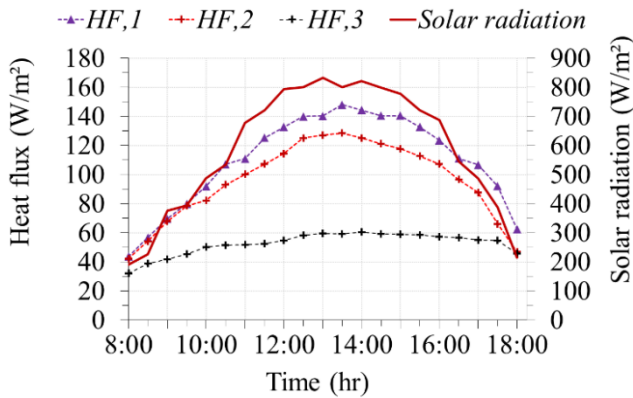


Figure 10. Hourly variation of ceiling heat flux in the three test rooms (Reference, Ventilated Grass Tray (VGT), and Multi-Tube Connected Ventilated Grass Trays (MCVGT)) in relation to solar radiation intensity

Figures 11–13 quantify these reductions in terms of percentage improvements. As shown in Figure 11, the VGT system achieved a heat flux reduction in the range of 14–22% relative to the reference room. This improvement corresponds to the reduced rooftop temperatures and weaker conductive heat transfer observed earlier in Section 4.1.2 and Section 4.1.3. Figure 12 highlights the incremental advantage of the MCVGT design over the VGT. The MCVGT achieved an additional 43–54% reduction in heat flux, which can be directly attributed to the system’s expanded ventilation network. By continuously flushing warmed air from the sub-tray cavity and facilitating lateral airflow between trays, the MCVGT prevents substantial heat buildup, resulting in lower conductive heat transmission to the ceiling surface. Figure 13 presents the total heat flux reduction achieved by the MCVGT system relative to the bare roof. Overall reductions ranged from 49–60%, with the highest values recorded during periods of peak solar irradiance. The strong correlation between solar radiation intensity and the magnitude of heat flux reduction confirms that the MCVGT system effectively responds to increased thermal loading by accelerating buoyancy-driven

airflow. Collectively, these findings demonstrate that the MCVGT configuration provides superior thermal performance compared with both the conventional VGT and the bare roof. The synergy of shading, substrate buffering, and enhanced sub-tray ventilation significantly limits conductive heat transfer into the building interior. This mechanism not only reduces heat gain but also directly contributes to lower indoor air temperatures and improved thermal comfort, as discussed in earlier sections. The results reaffirm the importance of integrating well-designed passive ventilation channels into modular rooftop greenery systems to maximize their thermal benefits in tropical climates.

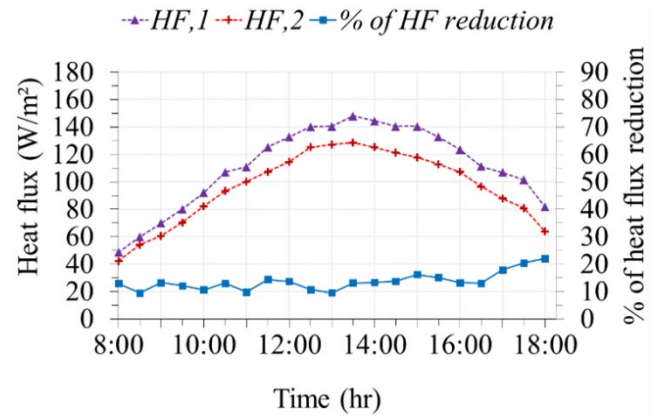


Figure 11. Percentage reduction in heat flux between the Ventilated Grass Tray (VGT) system and the reference room

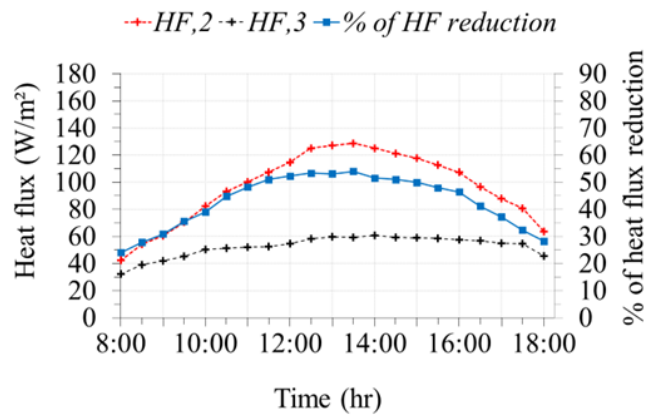


Figure 12. Percentage reduction in heat flux between the Multi-Tube Connected Ventilated Grass Trays (MCVGT) system and the Ventilated Grass Tray (VGT) system

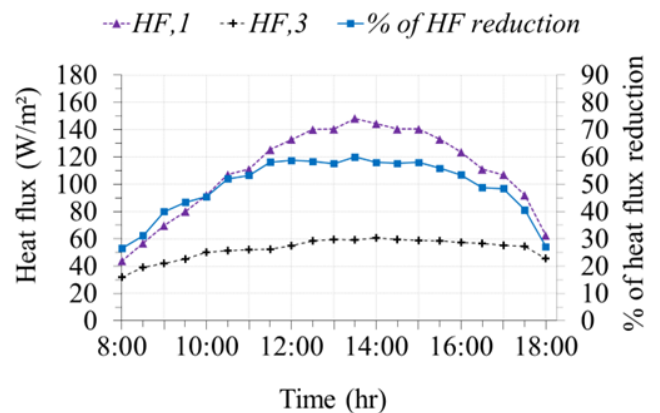


Figure 13. Percentage reduction in heat flux between the Multi-Tube Connected Ventilated Grass Trays (MCVGT) system and the reference room

4.4 Engineering implementation considerations

From an engineering perspective, the proposed grass tray systems are intended for application on lightweight building structures commonly found in tropical urban environments. The trays are fabricated from PVC foam board and contain a shallow planting layer, which results in relatively low self weight when compared with conventional green roof assemblies. This lightweight configuration allows installation on existing reinforced concrete or steel roof slabs without significant structural modification, provided that basic load capacity requirements are satisfied. Roof load considerations are particularly important under saturated conditions following irrigation or rainfall. The modular tray system distributes load uniformly across the roof surface, which reduces the risk of localized oversteering. As the planting depth is limited, the additional dead load remains within acceptable ranges for typical low rise and mid rise buildings in Southeast Asia.

Waterproofing performance is another critical implementation requirement. The grass tray systems are designed to be installed above a continuous waterproofing membrane, which isolates the structural roof slab from moisture penetration. Proper drainage beneath the trays is essential to prevent water ponding and to maintain long term waterproofing integrity. The ventilated air cavity beneath the trays further assists in moisture evaporation, which may reduce prolonged surface wetness. In terms of practical application, the modular nature of the VGT and MCVGT systems allows for ease of installation, maintenance, and replacement. The enhanced ventilation features of the MCVGT do not require mechanical components and therefore do not introduce additional operational energy demand or maintenance complexity. These characteristics support the feasibility of the proposed system for both new construction and retrofit projects in tropical urban buildings.

5. CONCLUSIONS

5.1 Key findings

This study experimentally evaluated the thermal and ventilation performance of two modular rooftop grass tray systems under real tropical outdoor conditions. The results demonstrate that the MCVGT system consistently outperformed the baseline VGT. The MCVGT reduced the average sub tray air temperature by 1.44 °C and lowered rooftop surface temperature by up to 3.00 °C compared with the bare roof condition. Ceiling heat flux was reduced by approximately 49 to 60 percent while indoor air temperature was maintained close to ambient levels. The enhanced system achieved air change rates exceeding 7 h⁻¹ during peak solar periods, whereas the VGT achieved approximately 2 h⁻¹.

5.2 Practical implications

The findings confirm that integrating engineered passive ventilation into modular grass tray systems significantly improves rooftop thermal reduction without mechanical energy input. The lightweight and modular configuration makes the MCVGT suitable for buildings with limited roof load capacity, which are common in tropical urban areas. The system can be applied as a passive cooling strategy to reduce

rooftop heat gain and mitigate indoor thermal loads in both new buildings and retrofit applications.

5.3 Future work

Future research should investigate long term system durability and plant performance under varying irrigation regimes and seasonal climatic conditions. Additional studies may also explore optimization of ventilation geometry, substrate composition, and integration with other passive rooftop systems such as rainwater management or urban agriculture functions.

ACKNOWLEDGMENT

The authors gratefully acknowledge the Innovation and Designing for Sustainability Program, Department of Architecture, Faculty of Architecture and Design, King Mongkut's University of Technology North Bangkok, for their valuable technical assistance and for providing the equipment required for the field experiments conducted in this study.

This research was funded by the Faculty of Architecture and Design, Contract No. Arch-Inter 01/2026.

REFERENCES

- [1] Mihalakakou, G., Souliotis, M., Papadaki, M., Menounou, P., Dimopoulos, P., Kolokotsa, D., Paravantis, J.A., Tsangrassoulis, A., Panaras, G., Giannakopoulos, E., Papaefthimiou, S. (2023). Green roofs as a nature-based solution for improving urban sustainability: Progress and perspectives. *Renewable and Sustainable Energy Reviews*, 180: 113306. <https://doi.org/10.1016/j.rser.2023.113306>
- [2] Li, W.C., Yeung, K.K.A. (2014). A comprehensive study of green roof performance from environmental perspective. *International Journal of Sustainable Built Environment*, 3(1): 127-134. <https://doi.org/10.1016/j.ijbsbe.2014.05.001>
- [3] Shahmohammad, M., Hosseinzadeh, M., Dvorak, B., Bordbar, F., Shahmohammadmirab, H., Aghamohammadi, N. (2022). Sustainable green roofs: A comprehensive review of influential factors. *Environmental Science and Pollution Research*, 29(52): 78228-78254. <https://doi.org/10.1007/s11356-022-23405-x>
- [4] Balasbaneh, A.T., Sher, W., Madun, A., Ashour, A. (2024). Life cycle sustainability assessment of alternative green roofs—A systematic literature review. *Building and Environment*, 248: 111064. <https://doi.org/10.1016/j.buildenv.2023.111064>
- [5] Abd Elrahman, A.S., Asaad, M. (2021). Urban design & urban planning: A critical analysis to the theoretical relationship gap. *Ain Shams Engineering Journal*, 12(1): 1163-1173. <https://doi.org/10.1016/j.asej.2020.04.020>
- [6] Wu, A.N., Biljecki, F. (2021). Roofpedia: Automatic mapping of green and solar roofs for an open roofscape registry and evaluation of urban sustainability. *Landscape and Urban Planning*, 214: 104167. <https://doi.org/10.1016/j.landurbplan.2021.104167>
- [7] Harada, Y., Whitlow, T.H. (2020). Urban rooftop agriculture: Challenges to science and practice. *Frontiers*

- in Sustainable Food Systems, 4: 76. <https://doi.org/10.3389/fsufs.2020.00076>
- [8] Nguyen Dang, H.A., Legg, R., Khan, A., Wilkinson, S., Ibbett, N., Doan, A.T. (2022). Social impact of green roofs. *Frontiers in Built Environment*, 8: 1047335. <https://doi.org/10.3389/fbuil.2022.1047335>
- [9] Triguero-Mas, M., Anguelovski, I., Cirac-Claveras, J., Connolly, J., Vazquez, A., Urgell-Plaza, F., Cardona-Giralt, N., Sanyé-Mengual, E., Alonso, J., Cole, H. (2020). Quality of life benefits of urban rooftop gardening for people with intellectual disabilities or mental health disorders. *Preventing Chronic Disease*, 17: E126. <http://doi.org/10.5888/pcd17.200087>
- [10] Daneshyar, E. (2024). Residential rooftop urban agriculture: Architectural design recommendations. *Sustainability*, 16(5): 1881. <https://doi.org/10.3390/su16051881>
- [11] Quddus, A. (2022). Rooftop gardening in the globe: Advantages and challenges. *Horticulture International Journal*, 6(3): 120-124. <http://doi.org/10.15406/hij.2022.06.00253>
- [12] Rawal, S., Thapa, S. (2022). Assessment of the status of rooftop garden, its diversity, and determinants of urban green roofs in Nepal. *Scientifica*, 2022(1): 6744042. <https://doi.org/10.1155/2022/6744042>
- [13] Barreca, F. (2016). Rooftop gardening. A solution for energy saving and landscape enhancement in Mediterranean urban areas. *Procedia-Social and Behavioral Sciences*, 223: 720-725. <https://doi.org/10.1016/j.sbspro.2016.05.248>
- [14] Li, H., Xiang, Y., Yang, W., Lin, T., Xiao, Q., Zhang, G. (2024). Green roof development knowledge map: A review of visual analysis using CiteSpace and VOSviewer. *Heliyon*, 10(3): e24958. <https://doi.org/10.1016/j.heliyon.2024.e24958>
- [15] Joshi, V.V. (2020). Heat transfer characterization of test rooms with six different roofs. *International Journal of Heat and Technology*, 38(1): 131-136. <https://doi.org/10.18280/ijht.380114>
- [16] Ananacha, T., Puangsombut, W., Hirunlabh, J., Khedari, J. (2014). Daylighting and thermal performance of thai modern façade wall. *Energy Procedia*, 52: 271-277. <https://doi.org/10.1016/j.egypro.2014.07.078>
- [17] Ghadikolaie, F.M., Ossen, D.R., Mohamed, M.F. (2020). Effects of wing wall at the balcony on the natural ventilation performance in medium-rise residential buildings. *Journal of Building Engineering*, 31: 101316. <https://doi.org/10.1016/j.jobe.2020.101316>
- [18] Ananacha, T. (2022). Thermal performance of the clear block wall for ventilation. *International Journal of GEOMATE, Geotechnique, Construction Materials and Environment*, 23(96): 25-31. <https://doi.org/10.21660/2022.96.3061>
- [19] Juengpimonyanon, K., Puangsombut, W., Ananacha, T. (2014). Field investigation on thermal performance of the tile ventilator. *Applied Mechanics and Materials*, 619: 73-77. <https://doi.org/10.4028/www.scientific.net/AMM.619.73>
- [20] Sungsoontorn, S., Nonthiworawong, D., Rattanadecho, P., Prommas, R. (2019). Experimental investigation of attic heat gain reduction and indoor illuminance using a light-vent pipe. *International Journal of Heat and Technology*, 37(4): 1171-1179. <https://doi.org/10.18280/ijht.370427>
- [21] Anan-archa, A., Chantawong, P., Khedari, J. (2023). Experimental and numerical investigation on design optimization of a roof skylight combined with solar chimney. *International Journal of Heat and Technology*, 41(3): 723-729. <https://doi.org/10.18280/ijht.410327>
- [22] Anan-archa, A., Chantawong, P., Khedari, J. (2022). A new configuration of roof skylight combined with solar chimney. *Journal of Engineering Research*, 1-17. <https://doi.org/10.36909/jer.16259>
- [23] Hou, M., Kong, X., Li, H., Yang, H., Chen, W. (2021). Experimental study on the thermal performance of composite phase change ventilated roof. *Journal of energy storage*, 33: 102060. <https://doi.org/10.1016/j.est.2020.102060>
- [24] Khedari, G., Chantawong, P., Ananacha, T. (2024). Enhancing indoor air quality and thermal comfort with a ventilated built-in closet design. *International Journal of Heat and Technology*, 42(6): 1963-1968. <https://doi.org/10.18280/ijht.420613>
- [25] Anan-archa, A., Ananacha, T. (2025). Heat accumulation reduction in condominium buildings using multi-typology rooftop landscapes. *International Journal of GEOMATE, Geotechnique, Construction Materials and Environment*, 29(136): 59-68. <https://doi.org/10.21660/2025.136.g15230>

NOMENCLATURE

<i>A</i>	cross-sectional area of ventilation opening, m ²
<i>ACH</i>	air change per hour, h ⁻¹
<i>Q</i>	volumetric airflow rate, m ³ /s
<i>T</i>	temperature, °C
<i>v</i>	air velocity through ventilation duct, m/s
<i>V</i>	volume of sub-tray air cavity, m ³
<i>HF</i>	heat flux, W/m ²
<i>SR</i>	solar radiation intensity, W/m ²

Subscripts

<i>Amb</i>	ambient air
<i>Avg</i>	average of temperature or velocity
<i>c1</i>	ceiling surface temperature under bare roof
<i>c2</i>	ceiling surface temperature under <i>VGT</i> system
<i>c3</i>	ceiling surface temperature under <i>MCVGT</i> system
<i>VGT</i>	Ventilated Grass Tray
<i>MCVGT</i>	Multi-Tube Connected Ventilated Grass Tray
<i>Inlet</i>	inlet position
<i>Outlet</i>	outlet position
<i>r1</i>	room temperature in reference room
<i>r2</i>	room temperature in <i>VGT</i> room
<i>r3</i>	room temperature in <i>MCVGT</i> room
<i>rt1</i>	rooftop surface temperature of reference room
<i>rt2</i>	rooftop surface temperature of <i>VGT</i> system
<i>rt3</i>	rooftop surface temperature of <i>MCVGT</i> system
<i>Ref</i>	reference test room